

REVIEW OF RECENT STUDIES OF THE
RADIATION INDUCED BEHAVIOR OF ION EXCHANGE MEDIA

K. SWYLER, R. E. BARLETTA, AND R. E. DAVIS

NOVEMBER 1980

PREPARED BY THE DIVISION OF
NUCLEAR WASTE MANAGEMENT
DONALD G. SCHWEITZER, DIVISION HEAD
DEPARTMENT OF NUCLEAR ENERGY
BROOKHAVEN NATIONAL LABORATORY
ASSOCIATED UNIVERSITIES, INC.
UPTON, NEW YORK 11973

Prepared for the U.S. Nuclear Regulatory Commission
Office of Nuclear Materials Safety and Safeguards
Contract No. DE-AC02-76CH00016

REVIEW OF RECENT STUDIES OF THE
RADIATION INDUCED BEHAVIOR OF ION EXCHANGE MEDIA

K. Swyler, R. E. Barletta, and R. E. Davis

Manuscript Completed: November 1980

Prepared by the Division of
Nuclear Waste Management
Donald G. Schweitzer, Division Head
Department of Nuclear Energy
Brookhaven National Laboratory
Associated Universities, Inc.
Upton, New York 11973

NOTICE: This document contains preliminary information and was prepared primarily for interim use. Since it may be subject to revision or correction and does not represent a final report, it should not be cited as reference without the expressed consent of the author(s).

Prepared for the U.S. Nuclear Regulatory Commission
Office of Nuclear Materials Safety and Safeguards
Contract No. DE-AC02-76CH00016
Fin No. A-3162

NOTICE

This report was prepared as an account of work sponsored by the United States Government. Neither the United States nor the United States Nuclear Regulatory Commission, nor any of their employees, nor any of their contractors, subcontractors, or their employees, makes any warranty, express or implied, or assumes any legal liability or responsibility for the accuracy, completeness or usefulness or any information, apparatus, product or process disclosed, or represents that its use would not infringe privately owned rights.

ABSTRACT

A review of the results of recent experiments on the effects of radiation on ion exchange media is presented. The results described include pH changes, gas generation, agglomeration of organic ion exchange resins and corrosion of mild steel in contact with ion exchange media.

CONTENTS

ABSTRACT.	iii
CONTENTS.	v
FIGURES	vi
TABLES.	vi
ACKNOWLEDGEMENTS.	vii
1. INTRODUCTION.	1
2. EXPERIMENTS PERFORMED AT GIT	3
2.1 Pressurization Experiments	3
2.2 Gas Content Experiments.	4
2.3 Agglomeration.	5
3. EXPERIMENTS PERFORMED AT PSU.	7
3.1 pH Changes	7
3.2 Agglomeration.	10
3.3 Gas Generation in Inorganic Ion Exchangers	11
3.4 Corrosion Studies.	12
4. EXPERIMENTS PERFORMED AT BNL.	15
4.1 Formation of Acid(s)	15
4.2 Agglomeration.	16
4.3 Corrosion.	16
4.4 Fast Electron Irradiations	17
5. SUMMARY OF RESULTS.	19
5.1 pH Changes	19
5.2 Gas Generation	20
5.3 Agglomeration.	20
5.4 Corrosion.	20
6. REFERENCES.	23
APPENDIX A.	25

FIGURES

1.1 Estimated Cumulative Dose to Epicor-II Ion Exchange Media as Used in TMI-2 AFHB Clean-up vs Time Based on Calculations of Appendix A. a-40 Ci-ft⁻³; b- 80 Ci-ft⁻³; c- 160 Ci-ft⁻³ 2

TABLES

2.1 Threshold Doses Observed During GIT Pressurization Experiments. . . 4

2.2 Maximum Gas Production Observed During Gas Generation Experiments at GIT. 5

3.1 Moisture Content and Initial pH of Resins Used in PSU pH Study. . . 8

3.2 Loading Patterns of Ion Exchange Columns for Buffering Action Experiments 8

3.3 pH Values of Solutions Formed From Irradiated Resins. 9

3.4 pH Values of Solutions Formed From Irradiation Ion Exchange Media . 9

3.5 Flow Rates Through Ion Exchange Columns Before and After ⁶⁰Co Irradiations. 10

3.6 Gas Generation in Zeolite (IONSIV-IE-95) During Irradiation 11

3.7 Corrosion Study Experiments 13

4.1 Hydrogen Ion Concentrations (as pH) of Water in Contact With Irradiated Ion Exchange Resins. 16

ACKNOWLEDGEMENTS

The authors would like to thank Drs. Donald G. Schweitzer, Thomas Gangwer, and Allen J. Weiss for many valuable discussions on aspects of the material reviewed. They also express their appreciation to Nancy Yerry for her skillful preparation in typing the manuscript.

REVIEW OF RECENT STUDIES OF THE RADIATION INDUCED BEHAVIOR OF ION EXCHANGE MEDIA

1. INTRODUCTION

Ion exchange materials are conventionally used to decontaminate water containing radionuclides. However, in the presence of ionizing radiation at high total absorbed dose (in excess of 10^6 rad), these organic ion exchange resins are known to undergo radiation damage. The previous work and some issues of the concerns for the short term storage of organic ion exchange resins containing high loadings of radionuclides based upon earlier literature were discussed in "Status Report on the Leachability, Structural Integrity, and Radiation Stability of Organic Ion Exchange Resins Solidified in Cement and Cement With Additives."⁽¹⁾ It was concluded in this report that the fundamental processes causing resin degradation are not understood and that the extent of radiation damage is specific to resin type.

Detailed information regarding radiation damage to ion exchange media pertinent to the conditions expected during the storage of ion exchange media waste generated in the auxiliary building (AFHB) cleanup activities at TMI-II is unavailable. Consequently, several scoping studies have been performed to estimate the magnitude of these problems. This work was conducted by R. C. Mc Farland at Georgia Institute of Technology (GIT),⁽²⁾ K.K.S. Pillay at Pennsylvania State University (PSU)^(3,4), and by the Division of Nuclear Waste Management at Brookhaven National Laboratory (BNL). Much of this work was performed using material typical of ion exchange media used in the nuclear industry since the identity of the actual ion exchange materials used in the EPICOR-II demineralizing system is not available at this time due to the vendor's concern over its proprietary nature. In the studies reviewed here, the investigators used external irradiation to simulate the radiation dose that is received by ion exchange media internally loaded with radionuclides. Differences in the radiation damage to ion exchange media have been observed in some cases for external as opposed to internal irradiation.⁽⁵⁾ While external irradiation simulates the most significant radiation effects, external irradiation does not simulate the actual radiation processes that occur with internal loading. This report is a review of the results of these scoping studies. We have arranged the body of the report, sections 2, 3, and 4, by the laboratory performing the work, rather than by the category of experiments even though similar or related experiments have been performed by more than one institution. The summary of results, section 5, groups the data by categories of experiments.

Figure 1.1 shows several estimated cumulative absorbed dose curves for Epicor-II ion exchange media as used in the TMI-II AFHB cleanup versus time. The bases of this figure are the results of the dose rate calculations outlined in the appendix of this report. These calculations assume that a total of 1300 curies of activity are uniformly distributed throughout the entire ion exchange bed volume (case a), one-half the bed volume (case b), and one-fourth the bed volume (case c). Within the considered volume, all of the beta particle energy is assumed to be deposited, while tissue equivalency is assumed for gamma ray

attenuation. If the more conservative approach of total gamma ray absorption was assumed, the total cumulative absorbed dose would increase by approximately a factor of two in comparison with the results given in Figure 1.1. Also, regions of high localized activity would result in a substantial increase in the cumulative dose delivered to these regions. The figure is included to allow the reader to make qualitative comparisons of delivered dose in the experimental work to a time frame.

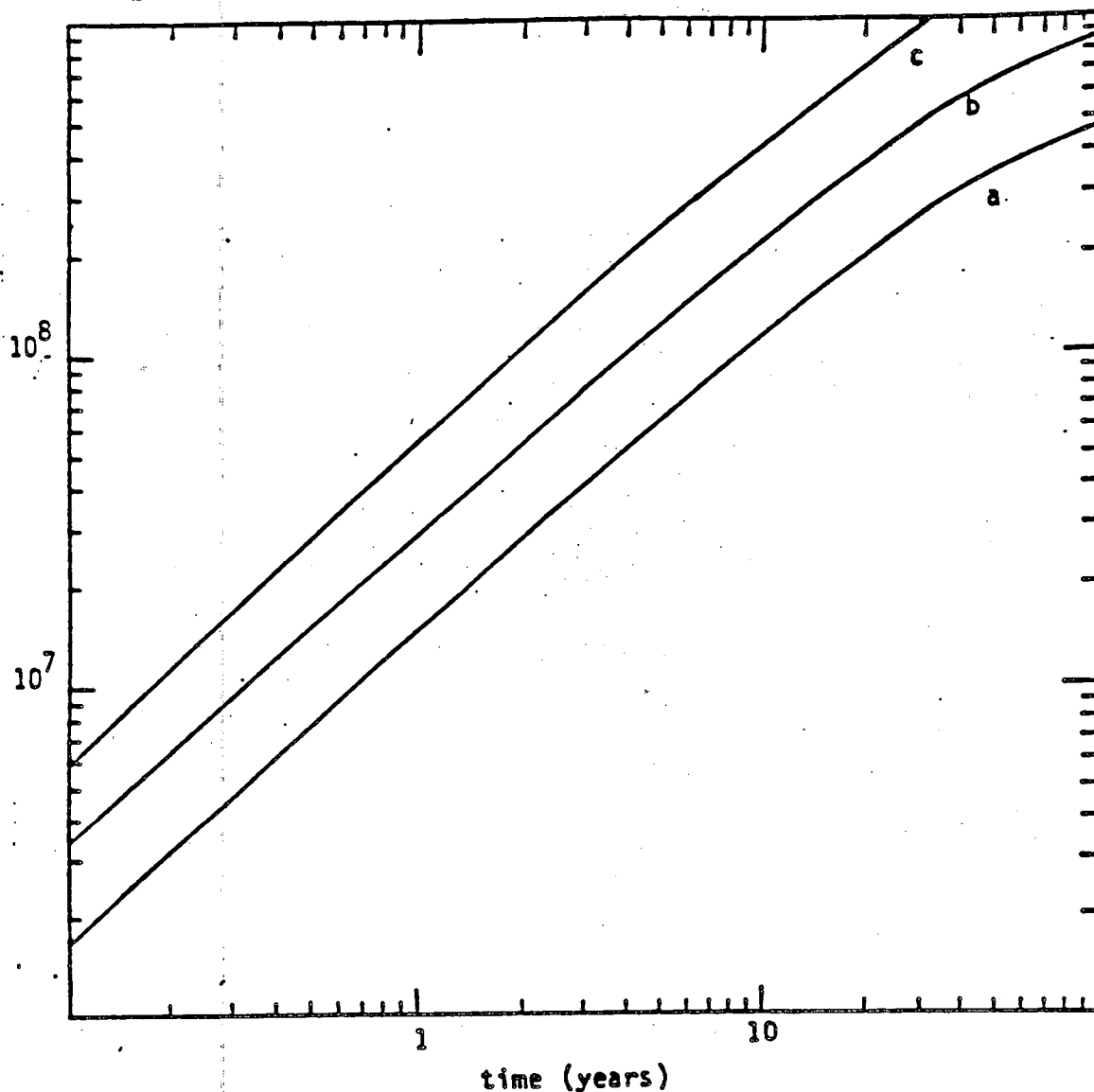


Figure 1.1 Estimated cumulative dose to Epicor-II ion exchange media waste as generated in the TMI-II AFHB cleanup vs time based on calculations of Appendix A.
a- $40 \text{ Ci}\cdot\text{ft}^{-3}$; b- $80 \text{ Ci}\cdot\text{ft}^{-3}$; c- $160 \text{ Ci}\cdot\text{ft}^{-3}$.

2. EXPERIMENTS PERFORMED AT GIT

The purpose of the experiments performed at GIT was to "determine the pressure buildup and gas composition as a function of gamma dose in burial canisters" of ion exchange media planned to be used in the TMI-II reactor building cleanup.⁽²⁾ This task was divided into two separate sets of experiments: pressurization and gas content. It should be noted that for the data in these experiments, experimental errors were not given, and these experiments were not originally planned in connection with the TMI-II AFHB cleanup.

2.1 Pressurization Experiments

The pressurization experiments were conducted on a cation ion exchange resin, an anion ion exchange resin, and activated charcoal irradiated in separate stainless steel capsules. The cation resin used was Dow HRC-S, and the anion resin used was Dow SBR-ON. These resins were converted to the sodium and borate forms respectively using a sodium borate solution (concentration and volume unspecified). The activated charcoal was also treated with the sodium borate solution. After this pretreatment, the samples were dewatered by pulling air through the column for two minutes. The samples were then placed in the irradiation capsules. A maximum of 66.79 cm³ of sample was placed in each capsule. This gave a void volume above the resin of about 10.33 cm³ (13.4%).

The capsules were then irradiated using a ⁶⁰Co gamma-ray source having a flux of approximately 5 x 10⁶ rad/hr. The maximum cumulative doses were approximately 2.5 x 10⁹ rad for the cation resin, 8 x 10⁸ rad for the anion resin, and 5 x 10⁹ rad for the activated charcoal. During the irradiation, air cooling was supplied to maintain the sample temperature between 30 °C to 45 °C.

In all cases, an apparent threshold for the onset of pressurization could be observed. Threshold values are given in Table 2.1. Both the cation and anion resins showed a linear increase in pressure with increasing dose above the threshold dose. The slope of this dose dependence was 0.083 psi/M rad for the cation resin (maximum dose of approximately 3 x 10⁹ rad) and 0.27 psi/M rad for the anion resin (maximum dose of approximately 8 x 10⁸ rad). The activated charcoal showed a rather different dose dependence. Above the threshold dose, the pressure rose rather rapidly to a maximum of about 5 psi at 1 x 10⁹ rad. Above 1 x 10⁹ rads, the pressure remained slightly below this peak value.

Table 2.1

Threshold Doses Observed During
GIT Pressurization Experiments (2)

Material	Cumulative Dose (rad)
Dow HRC-S	8×10^7
Dow SBR-ON	4.7×10^7
Activated charcoal	1.6×10^8

2.2 Gas Content Experiments

The composition of radiolytically generated gas as a function of dose was determined for the Dow HRC-S and the Dow SBR-ON resin. The resins were again pretreated with sodium borate. The samples were loaded into stainless steel capsules with a total volume of 18.9 cc. A single sample was run at each dose. (The dose rate was approximately 4.8×10^6 rad/hr.) After irradiation, the sample tubes were attached to an evacuated volume which contained a septum through which samples were withdrawn for gas chromatographic analysis.

A total of five gases were identified as cation resin degradation products: hydrogen, methane, ethane, propane, and butane. For the anion resin, hydrogen, methane, ethane, and propane were observed. In addition, traces of an unidentified hydrocarbon gas were detected in the high dose anion capsule. It was speculated by Mc Farland that this gas was a branched chain and/or unsaturated compound. Significant amounts of amines were not detected in either the cation or anion resin experiments.

The production of hydrogen, methane, ethane, propane, and butane (cation resin) was plotted versus total gamma dose. For H_2 and CH_4 , the production with dose appeared to be roughly linear for both cation and anion resins. While for the other gases, the dependence was more complex. The maximum volumes of gas generated per gram of resin estimated from Figures 10 through 14 of reference 2 are given in Table 2.2.

Table 2.2

Maximum Gas Production Observed During
Gas Generation Experiments at GIT⁽²⁾

Gas	Resin ^a	Amount of Gas mL/g	Dose (rad)
H ₂	cation	2.0 x 10 ⁻¹	3 x 10 ⁹
	anion	2.2 x 10 ⁻¹	5 x 10 ⁸
CH ₄	cation	2.1 x 10 ⁻²	3 x 10 ⁹
	anion	7.4 x 10 ⁻²	8 x 10 ⁸
C ₂ H ₆	cation	2.8 x 10 ⁻³	3 x 10 ⁹
	anion	1.3 x 10 ⁻³	8 x 10 ⁸
C ₃ H ₈	cation	6.4 x 10 ⁻⁵	1 x 10 ⁹
	anion	3.8 x 10 ⁻⁵	8 x 10 ⁸
C ₄ H ₁₀	cation	1.5 x 10 ⁻⁵	1 x 10 ⁹

^aCation resin Dow HRC-S and anion resin Dow SBR-ON.

2.3 Agglomeration

Although experiments were not specifically designed to provide any information on agglomeration, the following observations were reported:

- In the high dose samples, a liquid phase formed. The liquid phase had a volume approaching 50% of the original resin sample.
- Trapped gases in this liquid phase caused it to froth when the pressure was released. (4)

3. EXPERIMENTS PERFORMED AT PSU

The objective of the experiments performed at PSU was to initiate a preliminary scoping study aimed primarily at demonstrating speculated radiation induced behavior of ion exchange media and mild steel in contact with these media. In this regard, four areas were selected for this investigation: pH changes as a result of irradiation, agglomeration of ion exchangers, generation of gas from the radiolysis of an inorganic ion exchanger, and the corrosion of mild carbon steel in contacted with ion exchangers in a radiation field.

3.1 pH Changes

It is generally recognized⁽⁵⁾ that the radiation effects on ion exchange resins, as well as radiolysis of water within the resin matrix, produce a variety of products that significantly change the pH of the overall matrix. It was speculated that mixtures of cation exchangers in the hydrogen (H^+) form in combination with the ammonium (NH_4^+) form might produce a buffering action, due to the possible availability of NH_3 gas from the NH_4^+ form of the resin. The cation exchanger Amberlite IR-120 in the H^+ form was used as the primary material. A large batch of the NH_4^+ form of this resin was prepared by mixing a quantity of Amberlite IR-120 with NH_4OH . Layered combinations of these two forms of the cation exchanger with stratification ratios ranging from 1:10 to 1:1 to 10:1 by weight were used to examine this potential buffering action.

The initial pH and moisture content of the unirradiated resins are given in Table 3.1. Table 3.2 gives the column loading patterns used in the buffering experiment specimens. Specimen containers were made of quartz. All specimens were irradiated to a total absorbed dose of 7×10^7 rad in the gamma flux of a ^{60}Co source (at approximately 1.2×10^5 R/hr). After irradiation, columns were sectioned into approximately 2 gm samples. A 10 mL volume of deionized water was added to each sample, and the pH of the supernate was measured. The values of the pH are given in Table 3.3. A significant lowering of the pH was observed in all cases. For samples 25 and 27, a slight variation of pH along the height of column was seen.

The results of some additional pH measurements of irradiated ion exchange media are presented in Table 3.4. These specimen were gamma-irradiated to a total dose of 4.4×10^8 rad. Specimen containers for these experiments were made of aluminum. Since aluminum is reactive in either acid or alkaline environments, the observed pH values do not represent an accurate measure of the irradiated specimens acidity or alkalinity.

Table 3.1

Moisture Content and Initial pH of Resins Used in PSU pH Study⁽³⁾

Resin (form)	Moisture Content (%)	pH ^a
Amberlite IR-120 (H ⁺) ^b	39.7	3.4
Amberlite IR-120 (NH ₄ ⁺)	39.4	8.5
Amberlite IRA-400 (Cl ⁻) ^b	42.0	4.6
Zeolite (IONSIV-IE-95) ^b	0.0	8.0

^aThe pH was measured in the supernate of a mixture of 2 g of resin and 10 mL of deionized water (pH 6.8).

^bAs received from vendor.

Table 3.2

Loading Patterns of Cation Exchange Columns for Buffering Action Experiments⁽³⁾

Sample No.	H ⁺ Form	NH ₄ ⁺ Form
21	20 gms (bottom)	2 gms (top)
22	20 gms (bottom)	2 gms (top)
23	2 gms (top)	20 gms (bottom)
24	2 gms (top)	20 gms (bottom)
25	10 gms (bottom)	10 gms (top)
27	10 gms (top)	10 gms (bottom)

Table 3.3
pH Values of Solutions Formed From Irradiated Resins⁽³⁾

Section	Sample No.					
	21	22	23	24	25	27
Top						
1	1.6	1.6	2.2	2.1	2.1	1.5
2	1.6	1.6	2.1	2.1	2.0	1.5
3	1.5	1.5	2.1	2.1	1.9	1.5
4	1.5	1.5	2.2	2.1	1.8	1.6
5	1.5	1.5	2.2	2.2	1.7	1.6
6	1.5	1.5	2.3	2.3	1.6	1.7
7	---	1.5	2.3	2.3	1.6	1.8
8	1.5	1.5	2.3	2.3	1.6	1.9
9	1.5	1.5	2.4	2.4	1.5	2.0
10	1.5	1.6	2.3	2.5	1.5	2.1
Bottom						

^aThe pH was measured in the supernatant of a mixture of 2 g of resin and 10 mL of deionized water (pH 6.8).

Table 3.4
pH Values of Solutions Formed From
Irradiation Ion Exchange Media⁽³⁾

Ion Exchange	pH ^a
Amberlite IR-120 ^b	3.5
Amberlite IRA-400 ^b	4.6
IONSIIV-IE-95 ^c	9.0
IONSIIV-IE-95 + Amberlite-IR-120 + Amberlite IRA-440 ^d	4.0

^aThe pH was measured in the supernate of a mixture of 2 g ion exchanger and 10 mL of deionized water (pH = 6.8).

^bAs received from vendor.

^cDrip-dry.

^dEqual weights.

3.2 Agglomeration

Several columns containing single exchanger or layered beds of IONSIV-IE-95, Amberlite IR-120, and Amberlite IRA-400 were prepared in 2 cm diam x 20 cm long aluminium tubes. These ion exchange columns were then attached to a flow measurement system, and the flow rate of deionized water through the beds was measured. After allowing the excess water to drain out, the columns were capped with end fittings (not air-tight). These columns were then exposed to the gamma-flux in a ^{60}Co facility (4.5×10^6 R/hr) until the total dose received was approximately 2.2×10^9 rad.

After irradiation, the columns were again attached to the flow measurement device in the same way as before, and an attempt was made to measure the flow rate through the columns. Only the column filled with zeolite showed a flow. All of the columns containing organic exchanger showed no flow at all. These plugged columns were submerged in a large tank of water. In subsequent testing of the soaked columns flow was initiated in all but one case (IRA-400). The results of the flow testing are shown in Table 3.5.

Table 3:5
Flow Rates Through Ion Exchange Columns
Before and After ^{60}Co Irradiations⁽³⁾

Column No.	Ion Exchangers	Weight Ratio	Pre-irradiation flow rate (mL/min)	Post-irradiation flow rate ^a (mL/min)
1	IONSIV-IE-95	1	18	19 (without pre-treatment) see footnote
2	IONSIV-IE-95 & Amberlite IR-120	1:1	16	13
3	IONSIV-IE-95 & Amberlite IRA-400	1:1	19	22
4	IONSIV-IE-95 & Amberlite IR-120 & Amberlite IRA-400	1:1:1	12	11
5	Amberlite IR-120	1	23	25
6	Amberlite IRA-400	1	7	could not initiate flow

^aImmediately after irradiation, it was not possible to get any flow through the system under initial conditions. Flow was initiated by flooding the column and possibly creating flow channels.

3.3 Gas Generation in Inorganic Ion Exchangers

Zeolite (IONSIV-IE-95) samples of varying moisture content, some loaded with cesium, were exposed to ^{60}Co gamma radiation. These samples were placed in pyrex containers specially designed to allow subsequent study of gases produced within the matrix during irradiation.

The irradiation containers, with a volume of about 8 mL, were fitted with a "break-seal" and glass attachment to allow incorporation into a vacuum line for gas analysis. Known weights of zeolite samples were placed inside these glass containers, and they were heat-sealed at atmospheric pressure. The ratio of zeolite column volume to the total container volume was about 0.5. The samples were then exposed to ^{60}Co gamma radiation (at 3.9×10^5 R/hr) until a total dose of 1.4×10^8 rad was reached. Following the irradiation, the pressure was determined and the gas present in the samples was analyzed. The results are given in Table 3.6. The variations in gas compositions were attributed to the following reasons. "The well known ability of molecular sieves to adsorb significant amount of gases and the unique ability of zeolites to relatively retain large quantities of hydrogen account for the observed ratio of hydrogen and oxygen in the gas phase."⁽³⁾

Table 3.6
Gas Generation in Zeolite (IONSIV-IE-95)
During Irradiation⁽³⁾

Sample No.	Pretreatment ^a	Pressure (psi abs.)	Gases (volume %)		
			H ₂	O ₂	N ₂
31 ^b	Drip-dry	20.3	4.5	0.5	90.7
32	Drip-dry	18.0	1.3	32.5	66.2
33 ^b	Drip-dry	20.3	3.1	1.8	92.2
	(Cs-loaded) ^c				
34	Drip-dry	20.0	1.0	36.9	62.1
	(Cs-loaded) ^c				
35	Air-dry	13.9	0.9	29.2	69.9
36	Air-dry	---	0.6	24.1	75.4
37	Air-dry	13.0	1.0	33.1	66.0
	(Cs-loaded)				
38	Air-dry	11.6	0.6	33.4	66.1
	(Cs-loaded)				
Blank	Air-dry	13.9	---	20.2	79.8
	(non-irradiated)				

^aMoisture contents for air-dry and drip-dry zeolites were 21.0% and 33.3% (by weight), respectively.

^bMethane (3 to 4%) was identified in addition to H₂, O₂ and N₂. The source of methane is not understood.

^cThe Cs loading on these samples was 0.6 meq/g of dry zeolite.

3.4 Corrosion Studies

In order to ascertain the extent of radiation induced corrosion in ion exchanger systems, metal coupon studies were conducted. The ion exchange materials used were Amberlite IR-120, Amberlite IRA-400, and IONSIV-IE-95.

Two different types of irradiation facilities were employed for the corrosion experiments. One was a ^{60}Co gamma-irradiation facility. The other, a research reactor (TRIGA-Mark III) in the shutdown mode was used as the irradiation source having the fission product spectrum. Both single exchanger/coupon and layered bed exchanger/coupon systems were studied.

Mild steel coupons made from steel plates identified as ASTM-1018 grade were used in all the corrosion study experiments. This mild steel grade is similar in composition to other types of common steel such as ASTM-1020 and ASTM-A-36. All have a carbon content in the range of 0.20% to 0.25%. Finely polished coupons were prepared from one large piece of stock material. Irradiation experiments at ^{60}Co facility used coupons of size 12 mm x 50 mm x 3 mm. Another set of 12 mm x 30 mm x 3 mm coupons were used in irradiation experiments using the TRIGA Research Reactor. Blank samples (unirradiated) were prepared and preserved under identical conditions. The results of the corrosion experiment are summarized in Table 3.7.

The coupons from the blank samples showed little or no trace of rust or corrosion effects. The irradiated mild steel coupons were removed from the ion exchanger beds and were rinsed with water to remove the weakly attached resin beads adhering to the surfaces. These were then photographed (see reference 3) for the purpose of having a visual record. The corrosion layers on the specimen were then carefully removed using a nylon brush, and the weight losses of the mild steel coupons were determined. Some brief qualitative descriptions of the mild steel coupons, as they appeared before removing the crust formations on their surfaces, are also given in Table 3.7.

As is evident from the description in Table 3.7, all of the irradiated metal coupons showed significant corrosion. Pitting and corrosion were enhanced where the exchanger was directly in contact with the metal surface.

Table 3.7
Corrosion Study Experiments

Sample No.	Ion Exchangers Used	Irradiation Facility	Weight Loss % initial wt. mg/cm ²		Qualitative Features of Corroded Metal Coupon Surfaces
7	IONSIY-IE-95	60Co ^a	0.9	6.4	Spotty rusted areas with zeolite beads strongly adhering.
8	IONSIY-IE-95/ Amberlite IR-120	60Co ^a	2.6	19	One half covered with rust only. The other half had rust and resin beads.
9	Amberlite IR-120	60Co ^a	3.3	24	Covered with rust throughout. One end had white spots in addition to rust.
10	Amberlite IRA-400	60Co ^a	1.9	13	Uniform thin layer of rust. No crust formation.
11	IONSIY-IE-95/ Amberlite IRA-400	60Co ^a	4.4	32	No significant crust, but significant pitting on surfaces.
12	IONSIY-IE-95/ Amberlite IR-120/ Amberlite IRA-400	60Co ^a	4.1	30	Covered fully with black beads and rust.
7-B	IONSIY-IE-95	none	0	0	Bright surfaces. Barely visible rust spots at the edges.
9-B	Amberlite IR-120	none	0.3	2.0	Almost all of the surface of the coupon was covered with a very thin layer of corrosion product.
10-B	Amberlite IRA-400	none	0	0	Bright surfaces like the original sample. No visible corrosion products or rust spots.
41	IONSIY-IE-95	TRIGA ^b	0.5	3.1	Distinct, but spotty crust formation with zeolite particles adhering to the corrosion product.
42	Amberlite IRA-120	TRIGA ^b	3.5	27	Significant corrosion product build-up. Uniform throughout the surface.
43	Amberlite IRA-400	TRIGA ^b	0.7	5.2	Spotty corrosion product build-up, especially around edges of the coupon.
44	IONSIY-IE-95/ Amberlite-IR-120/ Amberlite-IRA-400	TRIGA ^b	0.8	6.2	Uniformly distributed surface layers of corrosion products.

^aDose = 2×10^9 rad; flux = 4.4×10^6 R/hr.
^bDose = 4.4×10^5 rad; flux = 7.6×10^5 R/hr.

4. EXPERIMENTS PERFORMED AT BNL

Radiation damage studies on organic ion exchange resins are currently underway at BNL. Using techniques similar to those discussed above, investigations of acid product formation (pH change), radiation induced corrosion, radiolytic gas formation, and resin agglomeration are being carried out. Irradiation facilities include a ^{60}Co gamma flux and a 3 MeV electron accelerator. The objectives of these experiments are first to confirm and extend the results of scoping studies described above, and, second, to determine the dependence of potentially significant radiation effects on key parameters such as radiation dose, dose rate, type of radiation and resin loading. To date, measurements have centered almost entirely on two resin types: the cation exchanger Amberlite IRN-77 and the "C-66%" resin supplied to BNL by the NRC. With the exception that C-66% is a cation exchanger, no written documentation is available.

The functional group on the IRN-77 resin is sulfonic acid ($-\text{SO}_3\text{H}$). This material is supplied in the hydrogen form. To investigate the sensitivity of radiation induced effects to resin loading, measurements were carried out on IRN-77 in the hydrogen form (IRN-77(H^+)) and on samples of IRN-77 which had been converted to sodium form (IRN-77 (Na^+)).

Certain preliminary results of the BNL investigations are described briefly in sections 4.1 through 4.4. It must be emphasized that these results are preliminary, and, in several cases, must be considered subject to confirmation. The objective here is to display early trends.

4.1 Formation of Acid(s)

A series of samples was gamma irradiated to various doses at a dose rate of approximately 4×10^6 R/hr. The irradiation were carried out in vented pyrex tubes. Following irradiation, the samples were thoroughly mixed with deionized water in the ratio 2 g resin to 10 mL water. The pH of the resulting solution was then measured and recorded. Initial results are shown in Table 4.1. Several observations are noteworthy:

- ① Without exception, for the resin studied, the pH steadily decreased for increasing gamma dose. This radiation induced generation of highly acidic conditions is in accord with previous measurements cited above.
- The acidity produced is sensitive to resin chemical loading. The sodium form of IRN-77 is much less acidic than the hydrogen form prior to irradiation, and this trend continues in irradiated samples. One sample of C-66% resin was titrated to pH 7 with NaOH prior to irradiation, which converted the resin to the sodium form. Following irradiation, the pH of the titrated C-66% resin solution was substantially higher than that of an untreated C-66% resin exposed to the same gamma dose.
- In the pH experiment, the water mixed with the irradiated resins becomes colored. The coloring darkens steadily from pale yellow to deep amber with increasing absorbed dose. For equal radiation doses, the coloring

was always more pronounced for IRN-77 (H⁺) than for IRN-77 (Na⁺). Thus, the coloring following the same qualitative trends shown in the pH measurements.

Table 4.1

Hydrogen Ion Concentrations (as pH) of Water in Contact With Irradiated Ion Exchange Resins

Dose (rad)	pH ^a			
	C-66%	C-66% (Na ⁺) ^b	IRN-77 (H ⁺)	IRN-77 (Na ⁺)
0	4.4	7.0	3.5	6.8
10 ⁷ (γ)	2.6	---	2.5	4.7
1.25 x 10 ⁷ (e ⁻)	---	---	2.5	---
3x10 ⁷ (γ)	2.0	---	2.0	3.6
4.6 x 10 ⁷ (e ⁻)	---	---	2.0	---
10 ⁸ (γ)	1.6	3.0	1.5	2.9
3 x 10 ⁸ (γ)	1.1	---	1.0	2.1
10 ⁹ (γ)	0.9	---	0.6	1.3

^aMeasured in supernate of a mixture of 2 g of resin and 10 mL of deionized water.

^bTitrated to pH 7 with NaOH prior to irradiation.

4.2 Agglomeration

Only qualitative results (visual observations) are presently available. For IRN-77 (Na⁺), IRN-77 (H⁺), and C-66% resins, irradiation to doses of approximately 10⁸ rad did not produce any severe agglomeration. The major visible effect was that the resins became progressively more colored. At 3 x 10⁸ rad, a definite stickiness was observable in all three resin types. The IRN-77 (H⁺) seemed most affected. At 10⁹ rad, the IRN 77 (H⁺) had a gummy appearance. The IRN-77 (Na⁺) was similarly agglomerated. The C-66% resin although quite sticky, was somewhat less agglomerated than IRN-77 (H⁺). When water was added to all these resins (10:2 by weight), the samples "deagglomerated". The IRN-77 (H⁺) formed a gel-like solution. Again, the C-66% resin seemed more durable.

4.3 Corrosion

Corrosion behavior of mild steel and stainless steel (304) in irradiated IRN-77 (H⁺), IRN-77 (Na⁺) and C-66% resins has been studied. Coupons were

imbedded in resin samples prior to gamma irradiation. The samples were then irradiated to various doses. Subsequently, the coupons were removed and compared with similar coupons which had been embedded in resins, but which received no irradiation. Again, at this point, only qualitative results are available. These are described below:

- For mild steel, corrosion was increased by irradiation. IRN-77 (H⁺) and C-66% resins appear more corrosive than IRN-77 (Na⁺).
- Corrosion is greater for samples irradiated to 3×10^8 rad than for those irradiated to 10^8 rad. The corrosion time for dose of 10^8 rad is approximately one day and three days at 3×10^8 rad dose.
- Thus far, (3 days corrosion time, 3×10^8 rad) radiation enhanced corrosion has not been observed for stainless steel.

4.4 Fast Electron Irradiations

Several samples of IRN-77 (H⁺) were irradiated with 2.2 MeV electrons. Both pH measurements in vented containers and gas evolution measurements in closed containers have been carried out. In the gas evolution measurements, the pressure was monitored while the irradiation progressed. The calculated dose based on beam current and energy loss data was approximately 1×10^8 rad per hour in the pressurization measurements and 5×10^7 rad per hour in the pH studies. Results to date indicate:

- The measured pH in the electron irradiation measurements so far agree reasonably well with the expected gamma irradiation at the same total dose (c.f., Table 4.1). This suggests that the pH change is not particularly sensitive to dose rate, and that electrons and gamma rays are sensibly equivalent on a per rad basis.
- At an absorbed dose of approximately 3×10^8 rad, an overpressure of about 3 psi was produced in the closed container experiment. We are presently determining the plenum volume; it is estimated at least 50%. The slope of the pressure versus dose curve appears so far to be closely proportional to radiation dose rate. This was determined by changing the beam current during irradiation, while monitoring the overpressure. This appears to be an extremely useful technique. Hydrogen and methane were identified as gaseous radiolysis products.

5. SUMMARY OF RESULTS

The work performed at GIT, PSU, and BNL described previously within this report fall into four categories: pH change, gas generation, agglomeration, and corrosion of metals in contact with irradiated ion exchange media. The results by category are summarized below.

No attempt was made to interpret the results of these experiments. This review is not intended to imply agreement with, or rejection of, the interpretations and conclusions given in the documents reviewed.

5.1 pH Changes

- For radiation doses of about 10^7 rad and above, all pH changes were observed by PSU and BNL to be substantial with respect to the pH of the unirradiated starting materials with the exception of IRA-400.
- The water added to irradiated resins to perform pH measurements at BNL was observed to become colored. The coloring darkens steadily (from pale yellow to deep amber) with increasing dose.
- Layered combinations of the H^+ and NH_4^+ forms of the IR-120 cation resins with stratification ratios ranging from 1:10 to 1:1 to 10:1 by weight were examined at PSU. All samples received 7×10^7 rad total absorbed dose. After irradiation all layered specimens had low pH values (1.5 to 2.5). Some specimens showed a modest variation of pH along the bed length. Based upon this experiment, the hydrogen form of IR-120 is estimated to have a final pH of 1.5, while the ammoniated form is estimated to have a final pH of 2.4.
- At PSU, the IRA-400 anion resin was irradiated to 4.4×10^8 rad, and had a measured final pH identical to that of the unirradiated starting material.
- Similar pH changes were observed at BNL for the IRN-77 H^+ form cation exchange resins to those changes observed at PSU for the IR-120 H^+ form at similar total accumulated total dose of about 10^8 rad. These irradiations were carried out in a ^{60}Co gamma flux. Several samples of resins irradiated at BNL to 10^9 rad showed pH values of about 1.0. Samples of the IRN-77 Na^+ form exchanger examined at BNL showed pH values consistently higher (less acidic) than the IRN-77 H^+ form.
- The electron irradiations of resins at BNL, which were about ten times higher in dose rate than the ^{60}Co irradiations, showed similar pH changes in the resins to those pH changes observed for gamma irradiated resin.

- The PSU study indicated that the final pH of the gamma irradiated zeolite increased from 8.0 to 9.0. The total dose for the zeolite specimen was 4.4×10^8 rad.

5.2 Gas Generation

- In the GIT study, significant quantities of gas were generated during irradiation of resins. Gas analysis identified the following components: hydrogen, methane, ethane, propane, and butane. An apparent threshold for the onset of pressurization varied from about 5×10^7 to 8×10^7 rad of cumulative dose for the various organic ion exchange media tested.
- At PSU, pressure changes indicating generation of gases were observed for the irradiated zeolite (1.4×10^8 rad dose).
- At BNL, gas generation was also observed in the electron irradiated resin experiments. Hydrogen and methane were identified as gaseous radiolysis products.
- GIT reported a liquid which frothed upon release of pressure which had developed in the sample container during the course of the irradiation. This observation suggests significant amounts of dissolved gas are present in the liquid.

5.3 Agglomeration

- Agglomeration of the resins was observed at GIT, PSU, and BNL. An attempt was made at PSU to evaluate the degree of agglomeration by measuring the flow rate of water through columns of packed ion exchangers before and after receiving gamma irradiation. At a dose of 2.2×10^9 rad, both the IR-120 cation (hydrogen form) and the IRA-400 anion resins had agglomerated to the degree that no flow of water could be observed. Irradiated zeolite specimens did not agglomerate.
- In the experiments at BNL, the addition of water was observed to "deagglomerate" irradiated resins.
- Georgia Tech reported a solid-liquid phase separation. Significant quantities of liquid were released from the irradiated resin matrix.

5.4 Corrosion

- Corrosion studies of metal coupons embedded in resins were performed at PSU. Irradiations were carried out in a gamma flux (either ^{60}Co or the mixed gamma-ray spectrum of the TRIGA-MARK III reactor in the shutdown mode). Substantial radiation induced pit-type corrosion was observed for mild steel coupons in all organic resin types, as well as the zeolite tested at doses from 4.4×10^8 to 2×10^9 rad.

- Recent work at BNL on corrosion of stainless steel imbedded in resins indicated no corrosion at the end of a three day experiment used to obtain a 3×10^8 rad dose.

6. REFERENCES

1. R. E. Barletta, R. E. Davis, T. E. Gangwer, M. Morcos, D. G. Schweitzer, and A. J. Weiss, "Status Report on Leachability, Structural Integrity and Radiation Stability of Organic Ion Exchange Resins Solidified in Cement With Additives," BNL-NUREG-28286 (1980).
2. R. C. McFarland, "The Effects of Gamma Radiation on Ion Exchange Resins and Activated Charcoal," TMI-II-RR-6 (1980).
3. K.K.S. Pillay, "Radiation Effects on Ion Exchangers Used in Radioactive Waste Management," NE/RWM-80-3 (1980).
4. T. Gangwer and K.K.S. Pillay, "Radioactive Loading of Ion Exchange Materials: Radiation Related Areas of Concern," BNL-NUREG-28647 (1980).
5. T. E. Gangwer, M. Goldstein, and K.K.S. Pillay, "Radiation Effects on Ion Exchange Materials, BNL-50781 (1977).

APPENDIX A

This appendix outlines the method used to calculate the cumulative absorbed dose as a function of time. The results of these calculations were displayed in Figure 1.1.

Table A.1 lists the radionuclides which were considered, as well as relevant quantities of activity and pertinent decay properties. The selection of these radionuclides and of the relative amounts was based upon an analysis of the influent to a particular TMI/EPICOR-II prefilter (#16). This information was obtained at a meeting held at the TMI site on October 20, 1980. The curies of an isotope were scaled such that a hypothetical liner would contain approximately 1300 total curies.

Table A.1

Nuclides and Relevant Decay Data Used in
Calculation of Dose Rates

Radionuclide ^a	Total ^b Curies	λ (yr ⁻¹)	$t_{1/2}$ (yr)	\bar{E}^c MeV	Γ^c (rad/cm ² hr ⁻¹ mCi ⁻¹)
⁸⁹ Sr	65	5.0	0.138	0.583	no γ ^d
⁹⁰ Sr	25	0.025	28	0.200	no γ
(⁹⁰ Y) ^e		(95)	(.0073)	(0.931)	(no γ)
¹³⁴ Cs	200	0.33	2.1	0.152	8.7
¹³⁷ Cs	1000	0.023	30	0.195	3.3

^aThese radioisotope accounted for approximately 99% of the total radioactivity.

^bNormalized to approximately 1300 total curies.

^cReference 6.

^dLess than 0.01% of ⁸⁹Sr decays with the release of a gamma ray; for the purpose of calculation this mode was neglected.

^eDaughter of ⁹⁰Sr; for the purpose of calculation, ⁹⁰Y was assumed to decay coincident with parent decay.

The remaining information (geometry, activity densities, etc.) used in the calculations is given in Table A.2. Three cases were considered. In each case, the total activity is assumed to be uniformly distributed throughout the volume of a cylinder. The radius of all cylinders is 60 cm, while the heights are 80, 40, and 20 cm. For these assumed geometries, the bulk activity densities are 40, 80, and 160 Ci/ft³, respectively.

The dose delivered by beta decay was calculated from the following equations. The initial beta dose rate of the *i*th radionuclide, D_i^β , is:

$$D_i^\beta = A C_i E_i$$

Table A.2

Assumed Geometry, Geometric Correction, and Activity Densities Used in Calculation

	a	Case b	c
radius (cm)	60	60	60
height (cm)	80	40	20
\bar{g} (cm ⁻¹)	216	206	180
volume (ft ³)	32.5	16.3	8.13
(cm ³)	9.2x10 ⁵	4.6x10 ⁵	2.3x10 ⁵
activity density, (mCi/cm ³)			
89Sr	0.07	0.14	0.28
90Sr	0.027	0.054	0.11
134Cs	0.22	0.44	0.88
137Cs	1.1	2.2	4.4

C_i is the activity density of the i th radionuclide, \bar{E}_i is the average beta energy and A is a proportionality constant. When C_i is in Ci/cm³ and \bar{E}_i is in MeV, A equals 2.1×10^3 rad cm³ MeV hr⁻¹mCi⁻¹ and D_i is obtained in rad per hr. The total absorbed beta dose due to the decay of the i th radionuclide, $D_i^{\beta}(\infty)$, is

$$D_i^{\beta}(\infty) = \frac{D_i^{\beta} \times 8.76 \times 10^3 \text{ hr}\cdot\text{yr}^{-1}}{\lambda_i}$$

where λ_i is the decay constant of the i th radionuclide in years⁻¹. The beta dose absorbed at any time may then be calculated by

$$D_i^{\beta}(t) = D_i^{\beta}(\infty) (1 - e^{-\lambda_i t}).$$

The dose delivered by gamma decay was estimated from the following equations. The gamma dose rate is

$$D_i^{\gamma} = C_i \Gamma_i \bar{g}$$

where Γ_i is the gamma ray constant of the i th radionuclide and \bar{g} is a geometric factor, which assumes tissue equivalency. Γ_i has the units rad cm²mCi⁻¹hr⁻¹; \bar{g} has the unit cm⁻¹.

The values of \bar{g} given in Table A.2 were estimated from the values of \bar{g} given in Reference 2. Extrapolation of \bar{g} for a cylinder of radius, r , of 60 cm was accomplished by least square fitting the published data to the form

$$\bar{g}^2 = mr + b.$$

The total gamma absorbed dose, $D_i^{\gamma}(\infty)$, is

$$D_i^{\gamma}(\infty) = \frac{D_i^{\gamma} \times 8.76 \times 10^3 \text{ hr}\cdot\text{yr}^{-1}}{\lambda_i}$$

and the cumulative gamma dose was obtained from

$$D_i^{\gamma}(t) = D_i^{\gamma}(\infty) (1 - e^{-\lambda_i t}).$$

The total cumulative absorbed dose for all nuclei and both decay types was obtained from the following equation,

$$D(t) = \sum_i (D_i^{\beta}(\infty) + D_i^{\gamma}(\infty)) (1 - e^{-\lambda_i t}).$$

This equation is plotted in Figure 1.1 as a function of time for each of the three loadings.

References

1. Bureau of Radiological Health and the Training Institute, Environmental Control Administration, Radiological Health Handbook, U.S. Government Printing Office, Washington, D.C. (1970).
2. G. J. Hine and G. L. Brownell, Radiation Dosimetry, Academic Press, Inc. New York (1956).